Bromide-mediated membraneless electrosynthesis of ethylene carbonate from CO_2 and ethylene

Menglu Cai [1,2,3], Siyun Dai [1,3], Jun Xuan[2,3] & Yiming Mo [1,3] ✉

Cyclic carbonates, such as ethylene carbonate, are crucial in various applications, including lithium-ion batteries and polymers. Traditional production routes for ethylene carbonate rely on high-temperature thermocatalytic processes that use fossil-fuel-derived epoxides and carbon dioxide (CO_2). Herein, we report a bromide-mediated membraneless electrosynthesis strategy for direction conversion of ethylene and CO_2 into ethylene carbonate. This method leverages electrolyte engineering to modulate the kinetics of solution chemistry to proceed at rates that match the high-current bromide electrooxidation, and cathode protection with chromium hydroxide film to suppress the parasitic bromine reduction reaction. These enable the system to operate at 10–250 mA/cm² current density with 47–78% Faraday efficiency towards ethylene carbonate. The system's practicality is underscored by achieving an ethylene carbonate product concentration of 0.86 M and maintaining stability for over 500 hours. Furthermore, we demonstrate the integration of this process with CO_2 electroreduction to ethylene, enabling a cascade ethylene carbonate electrosynthesis using only CO_2 and water as feedstocks. A comprehensive techno-economic analysis confirms the strong economic potential of this method for future applications.

As the world is moving towards a sustainable future powered by the renewable electricity, the surge in the use of lithium-ion batteries as the electricity storage media requires green and cost-effective routes to manufacture their required raw materials[1,2]. Cyclic carbonates, such as ethylene carbonate (EC) and propylene carbonate (PC), are the most widely used electrolytes in lithium-ion batteries[3,4]. The global production of EC, valued at $0.94 billion in 2023, is anticipated to nearly double to $1.49 billion by 2028[5]. However, existing industrial routes for EC production involve high-temperature (100–200 °C) and high-pressure (3.5–10 MPa) thermocatalytic reaction between epoxides and carbon dioxide (CO_2) (Fig. 1a)[6,7]. The corresponding feedstock ethylene oxide is derived from fossil fuels through the energy-intensive aerobic silver-catalyzed epoxidation process[6,8]. In light of the surging market demand for cyclic carbonates along with

the desired greener production, the development of sustainable and mild alternative synthesis methods is imperative.

Electrosynthesis driven by renewable electricity offers a sustainable route to access value-added chemicals[9,10]. Significant advances have been made to achieve electrocatalytic upgradation of gaseous feedstocks, such as the electrochemical conversion of CO_2 to C2+ hydrocarbons[11,12] and the ammonia synthesis via nitrogen electroreduction[13]. The selective electrochemical transformation of olefins to the corresponding epoxides, the intermediates for cyclic carbonates, has recently been advanced using various oxidative or reductive mechanisms, such as homogeneous halide-mediated[8,14] or heterogeneous Ag-catalyzed oxidative pathway using water as the oxygen source[15] and reductive pathway via gaseous dioxygen reduction-derived H_2O_2 to prepare epoxides[16]. However, the epoxides are still one step away from cyclic carbonates.

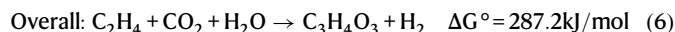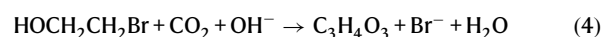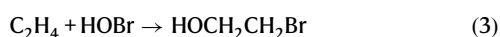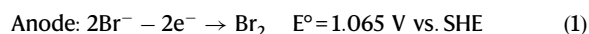[1]College of Chemical and Biological Engineering, Zhejiang University, Hangzhou, China. [2]Department of Chemistry, Zhejiang University, Hangzhou, China. [3]ZJU-Hangzhou Global Scientific and Technological Innovation Center, Zhejiang University, Hangzhou, Zhejiang, China. ✉e-mail: yimingmo@zju.edu.cn
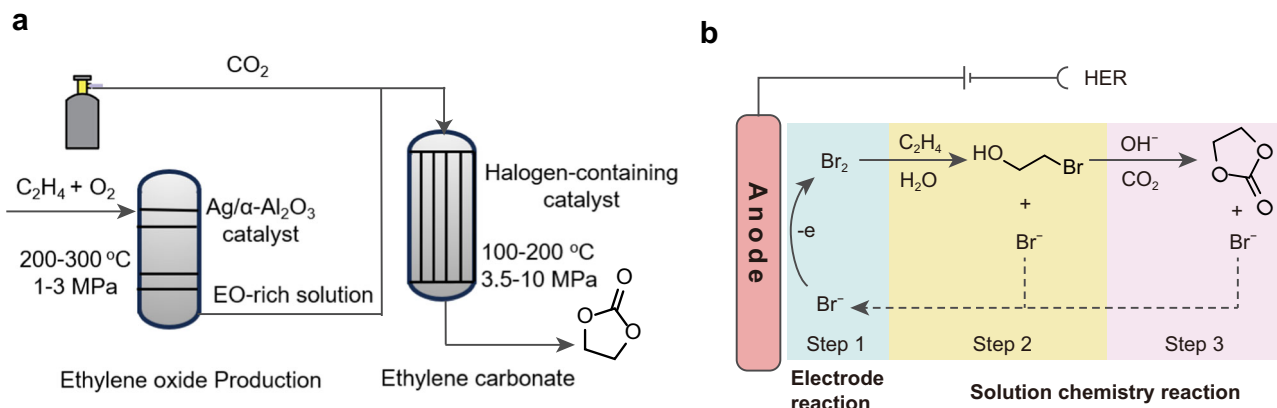
Fig. 1 | Routes for ethylene carbonate production. a Existing industrial thermocatalytic route for ethylene carbonate (EC) production. **b** The proposed bromide-mediated membraneless direct EC electrosynthesis strategy using ethylene and CO_2 as the feedstocks.

The direct electrosynthesis of cyclic carbonates still represents a straightforward approach to meet the requirement for sustainable synthesis. Dimethyl carbonate was electrosynthesized using CO_2 and methanol via a redox-neutral palladium-catalyzed pathway, achieving 60% Faraday efficiency (FE) at $12\,mA/cm^2$ current density[17]. Using widely available diols and CO_2 as the starting material for cyclic carbonate synthesis could proceed with electrogenerated base[18]. However, a stoichiometric amount of expensive tetraethylammonium iodide and iodomethane (Supplementary Table 1) were required as the supporting electrolyte and esterification reagent, respectively, and yields for various cyclic carbonates were generally lower than 60%. Similarly, with the help of electrogenerated base from cathodic hydrogen evolution, cyclic carbonates can be synthesized by reacting CO_2 with the corresponding epoxides at ambient conditions[19,20]. Nonetheless, to balance the charges used for cathodic base generation necessitates the anodic metal dissolution as the sacrificial electron donor. Alternatively, an oxidative pathway using iodide as the mediator can successfully convert aromatic and aliphatic olefins into the iodohydrin intermediates, which further react with CO_2 to obtain corresponding cyclic carbonates[21]. Its compatibility with gaseous olefins, such as ethylene and propylene, is yet to be validated (Entry 4 in Supplementary Table 2). Nam et al. reported a succinimide- and bromide-mediated cascade strategy for EC preparation, which was electrochemically driven for the initial bromine and base generation[22]. This strategy involved four separate reaction steps for the final EC synthesis, highlighting the need for a streamlined one-pot EC electrosynthesis method.

To pursue a practical cyclic carbonate electrosynthesis route under industrially relevant current densities (Supplementary Note 6), we here developed an electrochemical bromide-mediated membraneless synthesis strategy to convert readily available ethylene and CO_2 to EC under ambient conditions (Fig. 1b). Mechanistically, the anodically generated bromine/hypobromite reacts with the dissolved ethylene via halohydrin pathway to obtain 2-bromoethanol (2-BrEtOH) (Eq. (3)), which further undergoes intermolecular cyclization with CO_2 to form EC and regenerate bromide (Eq. (4)). The overall electrochemical conversion only requires ethylene, CO_2, and water as feedstocks to co-generate value-added EC and hydrogen (Eq. (6)).

$$\text{Anode: } 2Br^- - 2e^- \rightarrow Br_2 \quad E° = 1.065 \text{ V vs. SHE} \tag{1}$$

$$Br_2 + H_2O \rightleftharpoons HOBr + HBr \tag{2}$$

$$C_2H_4 + HOBr \rightarrow HOCH_2CH_2Br \tag{3}$$

$$HOCH_2CH_2Br + CO_2 + OH^- \rightarrow C_3H_4O_3 + Br^- + H_2O \tag{4}$$

$$\text{Cathode: } 2H_2O + 2e^- \rightarrow H_2 + 2OH^- \quad E° = -0.826 \text{ V vs. SHE} \tag{5}$$

$$\text{Overall: } C_2H_4 + CO_2 + H_2O \rightarrow C_3H_4O_3 + H_2 \quad \Delta G° = 287.2\,kJ/mol \tag{6}$$

The key to this efficient one-pot reaction design is modulating the reaction kinetics through electrolyte engineering, such that solution chemistry steps (Eqs. (2)–(4)) can proceed at high rates to match the high-current electrode reaction (Eqs. (1) and (5)). This direct EC electrosynthesis method is capable of operating at 10–$250\,mA/cm^2$ current density with 47–78% FE towards EC. Furthermore, the maximum concentration of the produced EC can reach 0.86 M (i.e., 7.6 wt%), thus significantly reducing the downstream separation cost. In addition, the electrosynthesis process can run stably for ~500 h without noticeable performance degradation. This bromide-mediated direct electrosynthesis approach can extend the starting olefin beyond ethylene to other olefins, including propylene and allylbenzene, to synthesize corresponding cyclic carbonates with high efficiency. Pursuing a carbon-neutral chemical production, we further developed a cascade system by integrating electrochemical CO_2-to-ethylene conversion and ethylene-to-EC electrosynthesis, thus achieving to use CO_2 and water as the only feedstocks for EC production. The techno-economic analysis of the developed electrochemical CO_2-to-EC process confirmed its potential for future practical application.

Results

Reaction design for electrosynthesis of ethylene carbonate

The overall reaction of using ethylene and CO_2 as the feedstocks to synthesize EC is an oxidative process that requires anode as the electron acceptor. Existing heterogenous activation strategies to achieve partial oxidation of alkene at anode are limited by their current density and selectivity[23–25]. In addition, the ethylene is potentially subject to overoxidation to aldehydes or even CO_2 as the complete oxidation products[26]. The state-of-the-art electrochemical heterogeneous olefin epoxidation achieved propylene conversion to propylene oxide with 66% FE at $50\,mA/cm^2$ current density on palladium-platinum alloy electrocatalyst[27]. However, FE for ethylene oxide electrosynthesis from ethylene reduced to 25% in this system due to the low electrophilicity of ethylene.

Here, we took an alternative approach that implemented a redox mediator to facilitate the selective and high-rate electron transfer between ethylene and anode, preventing the overoxidation of direct electrooxidation approach[8]. Conventionally, cyclic carbonate can be

synthesized from halohydrin and CO_2 through intermolecular cyclization[28,29], and the corresponding halohydrin can be prepared by the reaction between olefin and halogen or hypohalite[30]. However, this chemical route is seldom implemented in industrial production due to the consumption of stoichiometric amount of hazardous halogens. Inspired by the recent success of halide-mediated epoxide electrosynthesis[8], we postulated that direct electrosynthesis of EC can be also accomplished using a halide-mediated halohydrin pathway (Fig. 1b). However, the major challenge associated with this triple-step reaction in one-pot, which includes anodic halide oxidation, halohydrin formation, and intermolecular cyclization with CO_2, is the orchestration of their reaction kinetics in order to achieve a high productivity of EC (i.e., large current density with good FE).

Electrolyte engineering for one-pot ethylene carbonate electrosynthesis

We sought to modulate the triple-step reaction kinetics via electrolyte engineering, beginning with a detailed investigation and optimization of each individual step. First, with a brief survey of suitable halide mediator for this integrated EC electrosynthesis (Supplementary Fig. 1), we identified bromide (Br⁻) as the most effective mediator compared to chloride and iodide, achieving a 68% FE towards EC. Compared to Cl-mediated system, hypobromite could react with ethylene to form 2-BrEtOH at a much higher rate than hypochlorite, and bromide was a better-leaving group during cycloaddition (Eq. (4))[31–33]. For I-mediated system, no EC was generated, which was attributed to the sluggish disproportionation reaction of I_2 into hypoiodite[34].

To identify the optimal anode material for bromide oxidation reaction (BOR), various electrode materials, including IrO_2 based dimensionally stable anodes (IrO_2-DSA), platinum (Pt), carbon paper, and graphite, were investigated using linear scanning voltammetry (LSV) (Supplementary Fig. 2). IrO_2-DSA electrode has the lowest onset potential and largest current density for BOR, and the competing oxygen evolution reaction (OER) is unfavored at the oxidation potential of bromide (Supplementary Fig. 3). In bulk electrolysis, IrO_2-DSA also outperformed other electrode materials in terms of BOR FE (86%) and generated bromine concentration (21 mM) (Supplementary Fig. 4), and showed the highest Faraday efficiency for EC electrosynthesis (68% FE, Supplementary Fig. 5). Thus, IrO_2-DSA was selected the optimal anode material for the following study.

We next focused on engineering the kinetics of solution chemistries to match with electrode reaction. The proton or hydroxide ions are involved in the formation of 2-BrEtOH (Eqs. (2) and (3)) and EC (Eq. (4)), and thus, pH of the electrolyte would significantly impact the reaction kinetics (Fig. 2a). The ethylene to 2-BrEtOH formation rate decreased with increasing pH[30,32], and pH above 10 would totally inhibit the reaction possibly due to the lack of active HOBr species at high pH[35]. On the other hand, the nucleophilic cycloaddition of CO_2 and 2-BrEtOH to synthesize EC favors a basic electrolyte environment to the promote formation of the required alcoholate intermediate for the nucleophilic pathway[28]. Thus, a weakly alkaline environment (pH-8) would be ideal for both reactions (Eqs. (2)–(4)).

On the other hand, the nucleophilic CO_2 cycloaddition to 2-BrEtOH (Eq. 4) was sluggish in aqueous electrolyte (Fig. 2b), thus limiting its successful coupling with 2-BrEtOH formation for one-pot
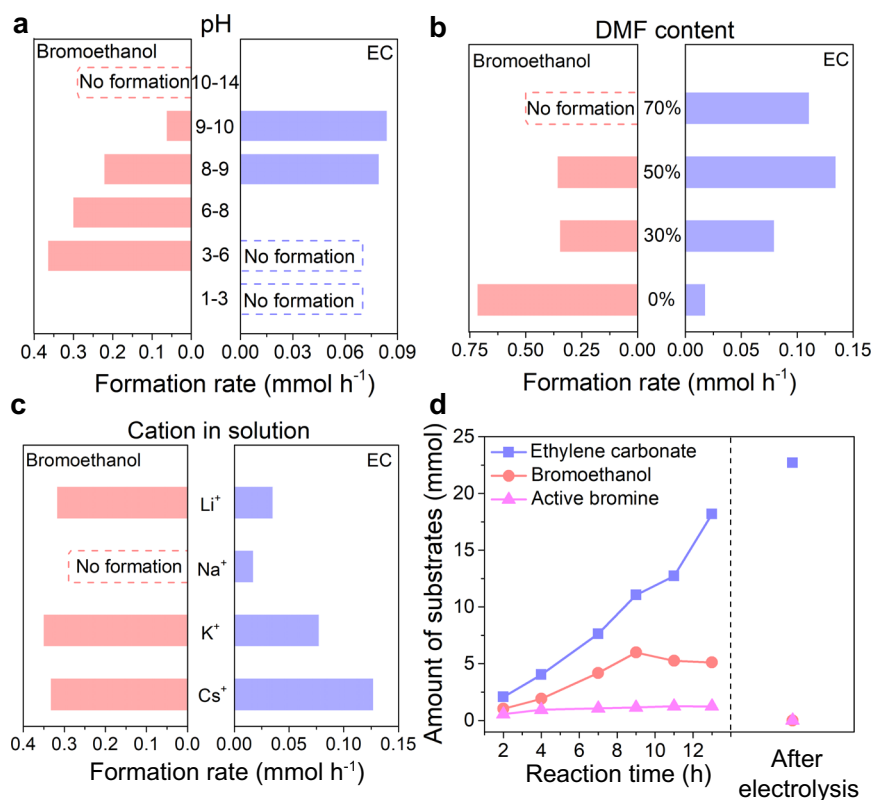
Fig. 2 | Investigation of the reaction kinetics through species balance and electrolyte engineering. Effects of (**a**) pH, (**b**) DMF content and (**c**) cations in solution on the formation of 2-BrEtOH and EC. For 2-BrEtOH formation, 0.5 M KBr, 0.2 M Cs_2CO_3, and 3 mM $K_2Cr_2O_7$ in 30 mL solvent with 30 sccm C_2H_4 supply at 20 mA/cm² current density for 30 min. IrO_2-DSA and nickel foam (2 cm²) was used as anode and cathode, respectively. For EC formation, adding 0.12 mmol $BrCH_2CH_2OH$ into 0.5 M KBr and 0.2 M Cs_2CO_3 in 3 mL CO_2-saturated DMF/water electrolyte, and the solution was shaken at 25 °C for 30 min in CO_2 atmosphere. For cation study, KBr and Cs_2CO_3 were replaced with corresponding cation bromides and carbonates. **d** Species concentration during electrolysis and when fully converted after stopping electrolysis. Reaction condition: 0.5 M KBr, 0.2 M Cs_2CO_3, and 3 mM $K_2Cr_2O_7$ in 120 mL DMF/water electrolyte (30:70 vol%) with 30 sccm ethylene and 80 sccm CO_2 supplying, and the reaction was performed under 20 mA/cm² with 7488C charges using IrO_2-DSA anode (8 cm²) and nickel foam cathode (8 cm²).
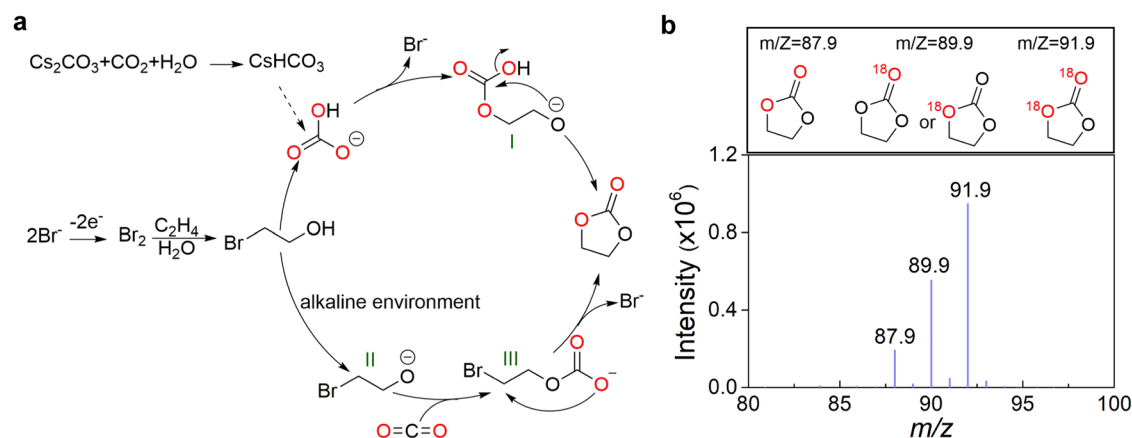
Fig. 3 | Investigation of the reaction mechanism. a Proposed reaction mechanism of EC in membraneless electrochemical cell. **b** The ^{18}O isotope experiments results. Reaction condition: 0.5 M KBr and 0.2 M Cs_2CO_3 in 3 mL CO_2-saturated DMF/ labeled $H_2^{18}O$ water electrolyte (30:70 vol%), and then 0.5 mmol of 2-BrEtOH was added and CO_2 was bubbled during the reaction.

EC electrosynthesis. To get around this kinetic barrier, aprotic polar organic solvent, such as dimethylformamide (DMF), was considered to expedite the CO_2 cycloaddition reaction[36]. Compared to aqueous electrolyte, 30 vol% DMF improved cycloaddition reaction rate by 4.5 times. A higher DMF content (>30 vol%) would limit the solubility of inorganic electrolytes (Supplementary Fig. 7a), which was unamenable for EC electrosynthesis in the electrochemical flow cells. However, DMF content in the electrolyte had a negative effect on 2-BrEtOH formation rate due to the inhibition of bromine disproportionation to hypobromite (Fig. 2b). Thus, the DMF/H_2O (30:70) mixture electrolyte solvent proved to be optimal after trading-off between reaction kinetics and electrolyte solubilities.

The alkali metal cations, including lithium (Li^+), sodium (Na^+), potassium (K^+), and cesium (Cs^+) were further investigated to fine tune the electrolyte environment (Fig. 2c and Supplementary Table 3). The type of cations had little effect on 2-BrEtOH formation rate, but significantly impacted EC formation rate (Fig. 2c). Due to the different nucleophilic strength during cycloaddition[29,37], Cs^+ showed the highest FE for one-pot EC electrosynthesis (Supplementary Table 3). However, considering the high price of CsBr (Supplementary Table 4), CsBr was replaced with the cheaper KBr, and this mixed cation electrolyte (KBr and Cs_2CO_3) gave similarly good performance as that of the Cs-only electrolyte (CsBr and Cs_2CO_3) (Supplementary Table 3).

The optimal electrolyte composition was 0.5 M KBr, 0.2 M Cs_2CO_3, and 3 mM $K_2Cr_2O_7$ in 30:70 vol% DMF/water. With this optimized electrolyte, the concentrations of 2-BrEtOH and EC (Fig. 2d) gradually increased during the early stage of the electrolysis, and after 9-hour electrolysis, 2-BrEtOH reached a plateau concentration while EC continued to accumulate, indicating a characteristic series reaction pattern. Continuing supplying CO_2 after stopping the electrolysis converted all remaining 2-BrEtOH to EC (Fig. 2d, Supplementary Fig. 10). In addition, an intermittent electrolysis experiment (Supplementary Fig. 11) revealed that the formation rates of 2-BrEtOH and EC were of similar magnitudes, confirming the desired outcome of electrolyte engineering on solution chemistry kinetics.

Reaction mechanism investigation
Next, we focused on elucidating the mechanism for conversion of 2-BrEtOH to EC (Eq. 4) since the halohydrin formation reaction mechanism has been extensively studied in existing literatures[8,32,38]. First, we sought to understand the reactivity of HCO_3^-, CO_3^{2-}, and dissolved CO_2 with 2-BrEtOH. Without the dissolved CO_2, HCO_3^- showed higher reactivity compared to CO_3^{2-} (Entries 1-2, Supplementary Table 5). In addition, supplying the electrolyte with CO_2 accelerated the formation of EC (Entries 3-4, Supplementary Table 5). Since

the cathodic HER would generate OH^- to react with CO_2 to form HCO_3^-, the concentrations of HCO_3^- and CO_2 should remain relatively unchanged during electrolysis. The pH of solution remained stable within 8.05-8.27 over the 13-hour electrolysis period (Supplementary Fig. 6). Thus, there are two plausible pathways occurring concurrently for the conversion of 2-BrEtOH to EC (Fig. 3a). (1) Reaction with HCO_3^-: the oxide anion of HCO_3^- undergoes nucleophilic addition to 2-BrEtOH with bromide as the leaving group, forming the corresponding bicarbonate intermediate (I). The intermediate I then converts to EC via the intramolecular cyclization[39,40]. (2) Reaction with dissolved CO_2: 2-BrEtOH first gets deprotonated in the alkaline electrolyte to form corresponding alcoholate (II), which attacks the dissolved CO_2 molecule to form a carbonate intermediate (III). This intermediate goes through the nucleophilic cycloaddition to obtain EC[28,37].

To further verify this reaction mechanism, we performed an ^{18}O isotope experiment using $H_2^{18}O$ as the ^{18}O source in the chemical conversion of 2-BrEtOH to EC (Supplementary Table 6). $CsHC^{16}O_3$ was first equilibrated in $H_2^{18}O$/DMF to ensure complete oxygen atom exchange between $CsHC^{16}O_3$ and $H_2^{18}O$[41]. Without supplying CO_2, GC-MS analysis of the resulting EC revealed three mass spectra peaks at 88, 90, and 92 m/z, corresponding to EC containing zero, single, and two ^{18}O atoms (Fig. 3b and Entry 1 in Supplementary Table 6). This indicated that EC has one oxygen atom from 2-BrEtOH, and the other two are from HCO_3^-, confirming the proposed HCO_3^- reaction pathway. If supplying the electrolyte with $C^{16}O_2$ (Entry 2 in Supplementary Table 6), the abundance of ^{16}O in the formed EC increased, suggesting participation of CO_2 in the EC formation, consistent with CO_2 reaction pathway.

Suppressing cathodic parasitic bromine reduction in membraneless electrolysis
The divided cell with a separating membrane provides an ion-selective transport or diffusion barrier for species in the electrolyte to avoid parasitic reaction of intermediates or products at the counter electrode[42]. But the associated cost, stability, and ohmic resistance issues of membranes diminish the advantages of electrosynthesis as a sustainable alternative for practical applications[43]. In the designed bromide-mediated electrosynthesis of EC, the anodically generated bromine is subject to the bromine reduction reaction (BRR) at the cathode, thus decreasing FE of the overall process. This parasitic BRR was confirmed by that FE for EC electrosynthesis in a divided with an anion-exchange membrane (82%) (Supplementary Fig. 12) was significantly higher than that in the undivided cell (55%) (Fig. 4a). Furthermore, reductive LSV scan of bromine-containing electrolyte showed a characteristic peak for BRR at −0.74 V vs. Ag/AgCl, which was
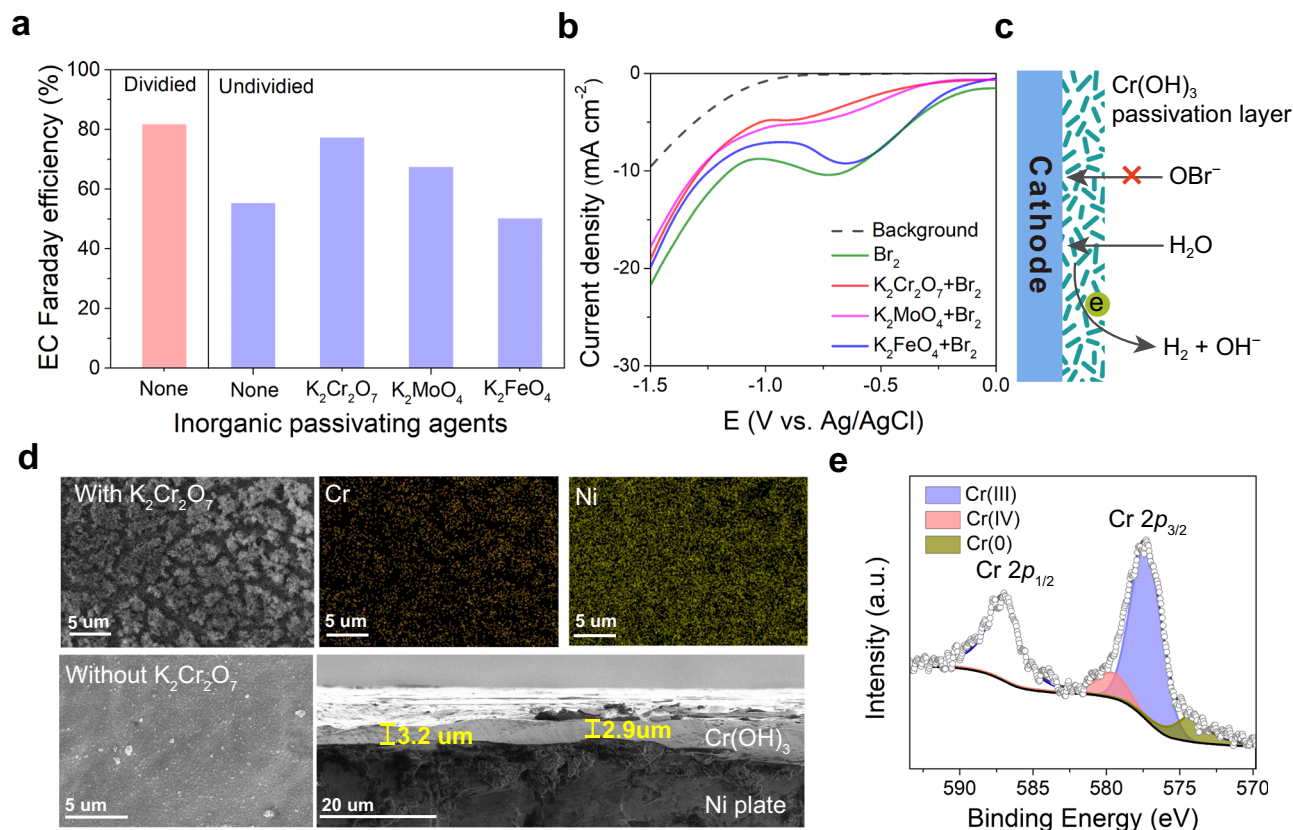
Fig. 4 | Suppression of parasitic bromine reduction reaction (BRR) on cathode in a membraneless electrochemical cell. a FE for EC electrosynthesis in divided and undivided cells. Reaction condition: 0.5 M KBr and 0.2 M Cs$_2$CO$_3$ in DMF-water (30:70 vol%) solution at 20 mA/cm^2 current density with IrO$_2$-DSA anode (2 cm^2) and nickel foam cathode (2 cm^2). For divided reaction, the reaction was performed in a flow-cell consisting of the IrO$_2$-DSA anode (2.25 cm^2), anion exchange membrane and nickel foam cathode (2.25 cm^2) at 20 mA/cm^2 current density. **b** The LSVs for cathodic BRR in presence of different additives (3 mM if added) performed in the CO$_2$-saturated DMF-water (30:70 vol%) solution containing 0.2 M Cs$_2$CO$_3$ and 0.01 M Br$_2$ (if added). Working electrode: IrO$_2$-DSA. Counter electrode: Nickel foam. Reference electrode: Ag/AgCl. **c** Schematics of BRR suppression mechanism. **d** Surface morphology and the corresponding EDS of the used nickel cathodes with and without K$_2$Cr$_2$O$_7$. **e** XPS spectra of the nickel plate cathode after being used for EC electrosynthesis in the electrolyte with K$_2$Cr$_2$O$_7$.

thermodynamically more favorable than hydrogen evolution reaction (HER, −1.06 V vs. Ag/AgCl) (Fig. 4b).

Using a shielding layer on the electrode surface to impose mass transfer limitation on thermodynamically more favorable reaction is an emerging strategy to overcome parasitic reactions[44,45]. The inorganic passivating agents (e.g., K$_2$Cr$_2$O$_7$, K$_2$MoO$_4$, and K$_2$FeO$_4$) are implemented in the chlor-alkali industry to improve FE towards sodium hypochlorite in the undivided cell[46,47]. Thus, we decided to investigate the effect of forming a similar shielding film on the cathode surface for suppressing BRR. A minor amount (3 mM) of K$_2$Cr$_2$O$_7$, K$_2$MoO$_4$, or K$_2$FeO$_4$ was added to the electrolyte for in-situ reductive formation of non-soluble metal hydroxide film, which could potentially serve as a selective diffusion barrier for bromine or hypobromite (Fig. 4c). LSV study revealed that the addition of K$_2$Cr$_2$O$_7$ and K$_2$MoO$_4$ could suppress the characteristic reduction peak of BRR (Fig. 4b), while K$_2$FeO$_4$ showed negligible impact on the behavior of BRR and HER. This BRR suppression effect was exemplified by the significantly improved FE for EC electrosynthesis in the membraneless electrochemical cell (Fig. 4a). The FE of EC was improved to 77% and 67% for electrolyte with K$_2$Cr$_2$O$_7$ and K$_2$MoO$_4$, respectively, close to that in divided flow cell. Consistent with the LSV analysis, K$_2$FeO$_4$ brought no benefits in suppressing BRR, but instead, slightly reduced FE to 50% possibly due to the instability of deposited Fe(OH)$_x$ in the bromine-containing electrolyte (Supplementary Fig. 14).

To probe the shielding mechanism, scanning electron microscopy (SEM) was used to study the morphology difference of the nickel plate cathodes with and without K$_2$Cr$_2$O$_7$ additive. When conducting EC electrosynthesis in a membraneless cell without any passivating additives, the originally smooth nickel cathode surface got severely corroded after the reaction (Fig. 4d and Supplementary Fig. 14b), which was attributed to the bromine corrosion of nickel cathode. Adding 3 mM K$_2$Cr$_2$O$_7$ resulted in a dense deposition of Cr(OH)$_x$ film, which had a 2.8-3.3 μm thickness (Fig. 4d). Energy-dispersive X-ray spectroscopy (EDS) confirmed the uniform dispersion of Cr on the nickel plate (Fig. 4d). X-ray photoelectron spectroscopy (XPS) was used to detect the Cr valence state (Fig. 4e). The peak at 587.2 eV and 577.5 eV corresponded to the Cr 2$p_{1/2}$ and Cr 2$p_{3/2}$ of Cr(III) species and were attributed to Cr(OH)$_3$. A minor amount of Cr(VI) and Cr(0) was also present, but Cr(III) species were dominant on the cathode surface, indicating Cr(OH)$_3$ hydroxide film was the main coating component after the electrolysis[48]. This porous Cr(OH)$_3$ shielding film served as a selective diffusion barrier to suppress the mass transport of negatively charged hypobromite anion via adverse potential gradient[46,49,50], while water molecules are still able to access the cathode surface (Fig. 4c).

Towards practical electrosynthesis of the ethylene carbonate

With the optimal electrode and electrolyte composition identified above for membraneless EC electrosynthesis, we next sought to explore its performance under practical current densities. The FE for EC reached 52% in a batch reactor at 20 mA/cm^2 current density (Supplementary Fig. 18). To boost the mass transport between the bulk electrolyte and electrode surface, a circulating electrochemical flow reactor was employed (Supplementary Fig. 19). The improved mass transfer allowed the current density to increase up to 250 mA/cm^2
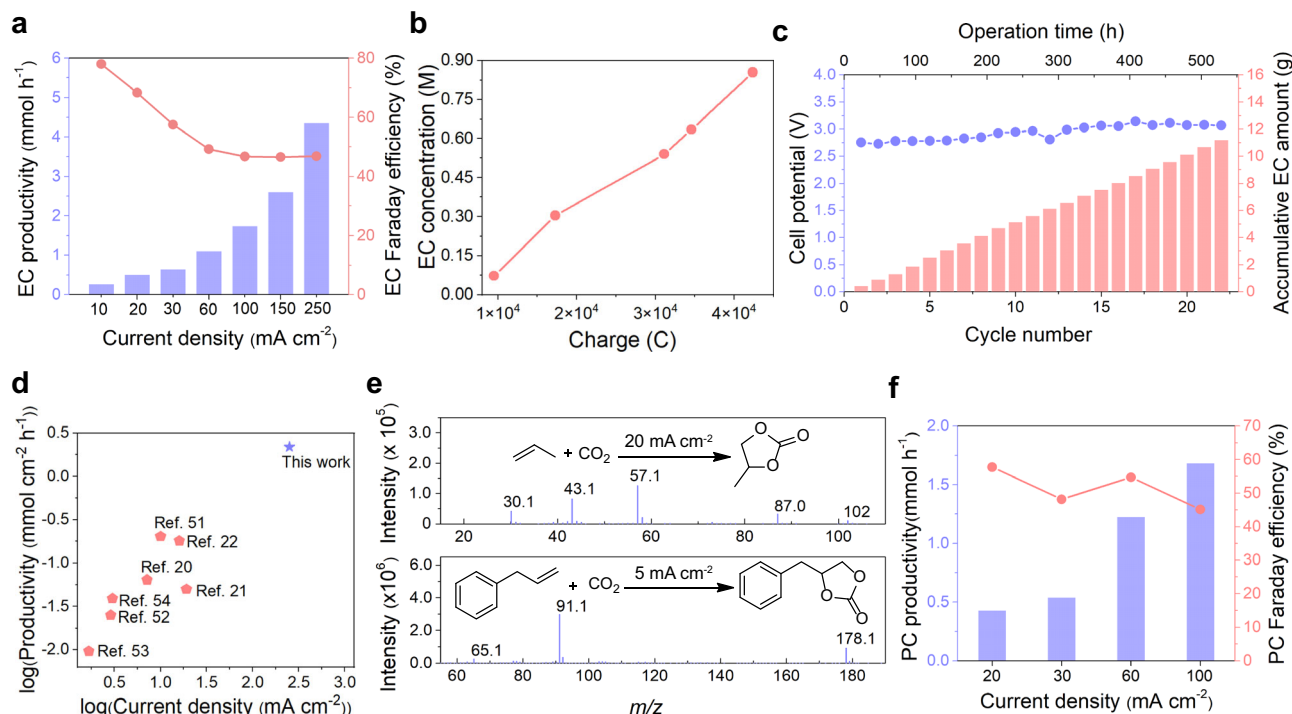
Fig. 5 | The performance of bromide-mediated cyclic carbonate electrosynthesis in a membraneless flow cell. a The productivity and FE of EC electrosynthesis under different current densities. **b** The concentration profile of EC in extended electrolysis at 30 mA/cm². **c** Stability study for EC electrosynthesis. Multiple batches of fresh electrolyte were sequentially electrolyzed at 20 mA/cm² for 13 h and continuing supply CO_2 for 11 h to ensure full conversion of the remaining active bromine and bromoethanol. Reaction conditions for (**a–c**): electrolysis performed in a flow cell (IrO_2-DSA anode and nickel foam cathode) using 0.5 M KBr and 0.2 M Cs_2CO_3 in DMF-water (30:70 vol%) solution with 30 sccm ethylene and 80 sccm CO_2 supply. **d** Comparison of current density and productivity for EC electrosynthesis with reported literatures. **e** Mass spectra of propylene carbonate and 4-(phenylmethyl)−1,3-dioxolan-2-one. **f** The productivity and FE values of PC at different current densities. Reaction conditions for (**e, f**): For PC, the electrolysis condition was same as the EC production, except that the substrate changes from ethylene to propylene. For allybenzene, 1 mmol of substrate was dissolved in 20 mL DMF-water (3:7 volume ratio) containing 0.2 M Cs_2CO_3, 0.15 M KBr, and 1 mM $K_2Cr_2O_7$. The flowrate for CO_2 supply was 40 sccm.

while still keeping a 47% FE (Fig. 5a). The EC productivity thus increased substantially, resulting in 8.6 times improvement to 4.4 mmol/h at 250 mA/cm² over the 0.51 mmol/h productivity at 20 mA/cm².

The product concentration in the reaction crude is one of the determining factors to the downstream separation cost. Our method could steadily increase the concentration of generated EC to 0.86 M (equivalent to 7.6 wt%) by extending the electrolysis time (Fig. 5b). This achieved concentration is significantly higher than that of the reported electrochemical EC synthesis method[19,21,51–53]. The stability of this electrochemical system was further investigated. Batches of fresh electrolytes were sequentially electrolyzed through the same flow reactor over the 550-hour stability test, during which the cell voltage remained stable at ~3.0 V and an accumulative 11.2 g EC was synthesized (Fig. 5c and Supplementary Figs. 20–22). While keeping the current density unchanged, we further scaled-up electrode area from 2 cm² to 8 cm², FE for EC in the large-scale flow cell was 74% similar to the small-scale, demonstrating the scaling potential of this strategy (Supplementary Figs. 23-24). Overall, our EC electrosynthesis strategy outperformed existing reported EC electrosynthesis methods in terms of system stability, EC concentration, current density, and productivity (Fig. 5d, Supplementary Fig. 25 and Supplementary Table 2)[19–21,51–54].

### Scope for electrosynthesis of cyclic carbonates
This strategy can also be adopted to produce other valued cyclic carbonates in addition to EC. Propylene carbonate (PC), an important electrolyte for lithium-ion batteries, could be prepared using propylene as the starting substrate. Performing the electrolysis at 20 mA/cm², a 0.43 mmol/h productivity and 58% FE was achieved.

Increasing the current density to 100 mA/cm² resulted in an improved PC productivity (1.7 mmol/h) with 45% FE (Fig. 5e, f). Going beyond gaseous olefins, the olefin substate with larger molecular weight, such as allyl benzene, can also undergo directly conversion to its corresponding cyclic carbonate with 82% yield (Fig. 5e). The demonstrated scope shows the potential of this bromide-mediated direct electrosynthesis method to be applied to other cyclic carbonates.

Techno-economic analysis and CO_2 emission of EC electrosynthesis
To evaluate the potential of this developed EC electrosynthesis method for future practical application, we conducted a techno-economic analysis (TEA) to assess the process economics (see detailed TEA calculation in Supplementary Note 1)[8,55]. Using the performance specifications of the developed EC electrosynthesis demonstrated above, the EC electrosynthesis from ethylene and CO_2 is able to produce EC at an estimated cost of US \$1379.9/ton under the existing electricity cost of US \$0.1/kWh[8]. Compared with the prices in the United States in March 2024[56,57], the production cost of EC electrolysis is lower than the \$2305/ton market price of EC (Fig. 6a and Supplementary Note 1). The value increase of the developed EC electrosynthesis demonstrates the strong economic driving force to implement this methodology in practice. Sensitivity analysis reveals that the electricity cost is major influencing factor for the EC electrosynthesis cost (Supplementary Fig. 30 and Supplementary Table 8).

Compared with the existing EC production routes based on fossil-fuel-derived EO feedstock[6,14], our electrosynthesis process could realize a lower CO_2 emission under the existing average grid CO_2 emission
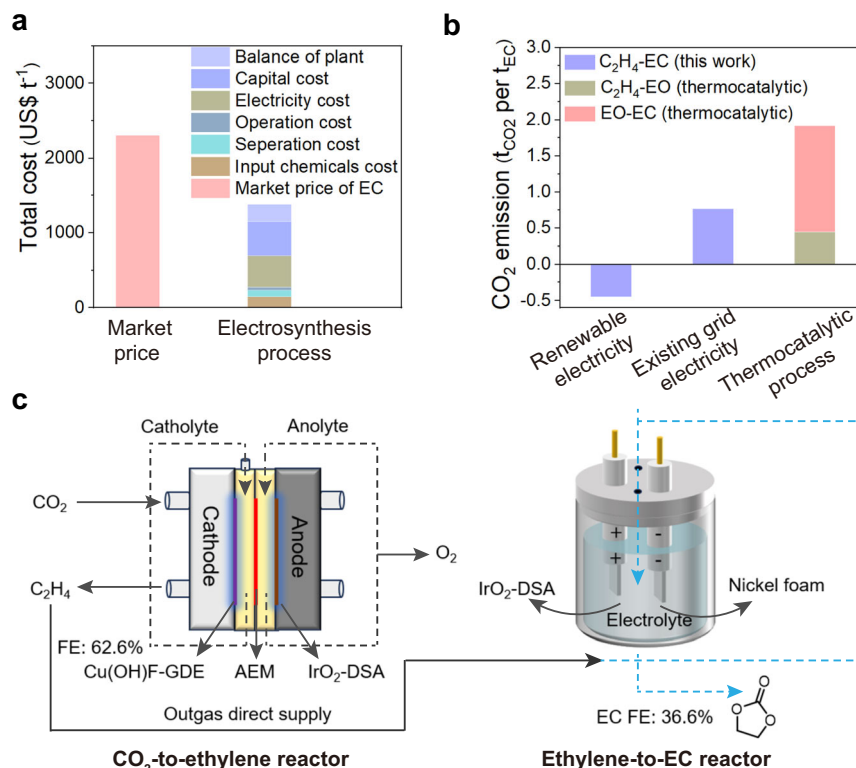
Fig. 6 | Techno-economic analysis and CO_2 emission of EC electrosynthesis, and cascade electrochemical CO_2-to-EC synthesis process. a Techno-economic analysis of single-step ethylene-to-EC electrosynthesis. **b** The comparison of the CO_2 emission for EC synthesis from ethylene using different production methods.

c Schematics of the two-stage cascade CO_2-to-EC system, including electroreduction of CO_2 to ethylene and bromide-mediated EC electrosynthesis using CO_2 and generated ethylene.

intensity (0.295 kg CO_2/kWh) based on the European Union's data (Fig. 6b and Supplementary Note 2)[10]. Furthermore, a negative CO_2 emission (consuming 0.45 ton of CO_2 per ton of EC produced) can be achieved when using renewable electricity as the energy source (Supplementary Note 3-4)[58]. This underscored the potential of the developed method in future shift towards carbon-neutral chemical production using renewable energy.

Cascade ethylene carbonate production from CO_2 and water

The current industrial route for EC uses the fossil fuel derived ethylene as the starting feedstock. To further reduce the carbon footprint of the overall EC production process, we sought to develop an integrated electrochemical system, relying on CO_2 and H_2O as the only feedstocks to synthesize EC. Our integrated system involves a two-step cascade electrochemical conversion. In the initial stage, within an electrochemical flow reactor with gas diffusion electrode (GDE), CO_2 was reduced to ethylene, which was then channeled into the subsequent EC electrosynthesis stage. This system provides a route to use renewable electricity for converting CO_2 and H_2O into a valuable commodity chemical.

In detail, for CO_2 electroreduction, sheet-shaped copper fluoride hydroxide (Cu(OH)F) nanoparticles were used as the electrocatalyst for selective conversion of CO_2 into ethylene (Supplementary Figs. 26–28)[59]. When operating at 100 mA/cm^2, a $63 \pm 4\%$ C_2H_4 FE was achieved. To obtain sufficient supply of ethylene for the second EC electrosynthesis step, an electrolyzer with 5 cm^2 electrode area was constructed to convert 5 sccm CO_2 inlet steam into an outlet gas mixture containing 0.016 mmol/min ethylene. This outlet stream was directly sparged, without intermediate purification, into a batch cell for the subsequent EC electrosynthesis (Fig. 6c). Operating the EC electrosynthesis at a 6 mA/cm^2 current density, 37% FE was achieved.

The lower FE compared to previous single-step EC electrosynthesis was primarily due to the low ethylene flowrate generated by 5 cm^2 electrolyzer for CO_2 electroreduction, which was confirmed by directly sparging the electrolyte with 0.09 mmol/min ethylene mixed in 5 sccm CO_2 leading to an increased FE of 46% (Supplementary Fig. 29). If perform CO_2 to ethylene conversion at large scale, distillation[60,61] and other emerging methods like physisorption[60,62,63] and membrane separation[64] can be used for ethylene separation, which is beneficial for improving the downstream EC electrosynthesis FE and current density.

For the integrated cascade EC synthesis using CO_2 and water as the feedstock, the production cost increased to US \$2326/ton due to the high cost of C_2H_4 electrosynthesis using existing technology and electricity cost (US \$0.1/kWh), which was consistent with the reported analysis (Supplementary Note 7)[10]. Considering that the electricity cost continues to decrease along with future development of the CO_2-to-C_2H_4 electrosynthesis process, the production cost of the integrated cascade CO_2-EC system is projected to drop to US \$1275/ton under US \$0.04/kWh electricity cost (Supplementary Fig. 31 and Supplementary Note 8)[10]. When using renewable electricity to power the cascade EC electrosynthesis, the CO_2 emission for electricity generation is 0.01 t/MWh[58], based on this parameter the CO_2 emission was only -1.39 ton_{CO2}/ton_{EC}, lower than the -0.46 ton_{CO2}/ton_{EC} CO_2 emission when using fossil-fuel-derived ethylene in the single-step EC electrosynthesis method above (Supplementary Fig. 32 and Supplementary Note 4, 10).

Discussion

In summary, we have demonstrated an electrochemical bromide-mediated EC synthesis directly from ethylene and CO_2 in a membraneless flow cell. Using an IrO_2-DSA as the anode and nickel foam as the

cathode, 47–78% FE towards EC was achieved at 10–250 mA/cm² current density with 0.27–4.4 mmol/h productivity. Prolonging the electrolysis time, the EC concentration could reach to 0.86 M. Furthermore, this system has shown an excellent stability, maintaining stable for over 500 h with negligible performance degradation. This method could extend to other olefin substrates to synthesize corresponding valued cyclic carbonates. We also developed a cascade system for EC production, which coupled EC electrosynthesis with CO₂ electroreduction to ethylene, achieving to use CO₂ and water as the only feedstocks for EC synthesis. The corresponding techno-economic analysis and CO₂ emission assessment illustrated its potential for a cost-effective and environmentally sustainable pathway to EC synthesis.

Methods

Materials and chemicals

The IrO₂-DSA electrode (thickness 1 mm, 15 mm × 25 mm) used for anodic bromide oxidation was purchased from Shengbailong and the content of IrO₂ is around 10–15 g/m². The nickel foam (thickness 1 mm, 15 mm × 25 mm) electrode used as cathode for C₂H₄-EC production. The conductive polypropylene (PP) plate (thickness 1 mm) was purchased from Nake. Carbon gas-diffusion electrode (YLS-30T) for CO₂ electroreduction, and anion exchange membrane (FAB-PK-130) used in CO₂ electroreduction were purchased from Suzhou Sinero Technology. The Ag/AgCl (φ = 4 mm) was purchased from Xianfengyiqi with 3 M KCl as the electrolyte. The Nafion D520 polymer binder solution (5 wt%) was purchased from SCI Materials Hub. Chemicals used, such as KBr (AR 99%), Cs₂CO₃ (AR 98%), K₂Cr₂O₇(AR 99.8%), DMF (AR 99.5%), CsBr (AR 99%), CsHCO₃(99.9%), Cu(NO₃)₂·2H₂O (AR 99.0%) and NH₄HF₂(AR ≥ 98%), were purchased from Sinopharm Chemical Reagent and Macklin, and used without further purification. CO₂ (99.99%) was purchased from Hangzhou Mingxinghuagong and C₂H₄ (99.9%) was purchased from Hangzhou Jingongwuzi.

Characterization and product analysis

The morphologies of the electrode were investigated through SEM (Thermo Fisher Scientific, Scios2 Hivac) equipped with an Oxford Xplore 50 EDX detector. The X-ray diffraction (XRD) was performed on an X-ray diffractometer (Bruker, D2 PHASER). The surface chemical composition of prepared samples was obtained by X-ray photoelectron spectroscopy (XPS) on a Thermo Fisher Scientific K-Alpha spectrometer using Al Kα radiation (1486.6 eV). C 1s peak (BE = 284.8 eV) was used as the reference to calibrate the XPS data.

The linear sweep voltammetry (LSV) was conducted on a three-electrode setup with Ag/AgCl (3M KCl) as the reference electrode at a scan rate of 20 mV/s (CHI1140C potentiostat). Unless otherwise specified, the test is a static test at room temperature, and the test room maintains at about 25 °C all year round.

The product yield was determined by gas chromatography-mass spectrometry (GC-MS, Agilent 8890-5977B) using naphthalene as the internal standard or high-performance liquid chromatography (HPLC, Agilent 1260) with a refractive index detector (RID) using n-butyl alcohol as the internal standard. Before GC-MS analysis, EC was extracted three times using ether-dichloroethylene (1:5) from the reaction solvent to avoid injecting nonvolatile salts into GC-MS system. ¹H NMR spectra were recorded on a Bruker 600 MHz NMR spectrometer in DMSO-d6 with mesitylene as the internal standard.

Procedure for electrosynthesis of cyclic carbonates

For bromide-mediated EC electrosynthesis experiment, we used a membraneless flow cell as the reactor (Supplementary Fig. 19), which was equipped with a porous IrO₂-DSA anode (2 cm² in size and 1 mm thick) and a nickel foam cathode (2 cm² in size and 1 mm thick). The flow rate of CO₂ and C₂H₄ was controlled by mass flow controllers (CS200-A, Beijing Sevenstar Flow), and was set to 80 sccm and

30 sccm, respectively. 0.2 M Cs₂CO₃, 0.5 M KBr and 3 mM K₂Cr₂O₇ dissolved in 30 mL DMF-water blended solution (3:7 volume ratio) was used as the electrolyte for EC electrosynthesis. Before electrolysis, the solution was saturated by CO₂, and then circulated through the flow cell with a 10 mL/min flowrate using a peristaltic pump (L100-1S−2, Longer). A constant current (10–250 mA/cm²) was applied for a designated reaction time at ambient temperature, and continuing supply CO₂ after stopping the electrolysis to consume all remaining bromine and 2-BrEtOH to EC. The product samples were analyzed by GC-MS with naphthalene as the internal standard. The 2-BrEtOH was analyzed by HPLC with n-butyl alcohol as the internal standard using RID. The electrosynthesis setup and operating parameters of propylene carbonate were the same as that of EC electrosynthesis, except for the ethylene feedstock was replaced with propylene.

For the electrochemical conversion of liquid olefins, 1 mmol of substrate was dissolved in 20 mL DMF-water electrolyte (3:7 volume ratio) composed of 0.2 M Cs₂CO₃, 0.15 M KBr, and 1 mM K₂Cr₂O₇. The flowrate for CO₂ supply was 40 sccm, and electrolyte was circulated at 10 mL/min. The electrolysis was carried out at ambient temperature until 3 F/mol electrons were supplied. The reaction crude was washed with saturated NaCl aqueous solution, and then extracted with ethyl acetate for three times. The organic layers were combined and then dried with anhydrous Na₂SO₄. Unless otherwise stated in the figure legend, all data are from one run. The yield was calculated based on the ¹H NMR with mesitylene as the internal standard.

Unless otherwise state in the figure legend, the FE value towards cyclic carbonate was calculated from one experiment as follows:

$$FE = \frac{nNF}{Q} \tag{7}$$

where n is the number of electrons transferred, N is the molar quantity of cyclic carbonate synthesized, F is Faraday constant, and Q is the total charged passed.

Preparation of Cu(OH)F-GDE catalyst

The copper-based catalyst for CO₂ reduction was synthesized using a hydrothermal method according to the literature[59,65]. 4 mmol of Cu(NO₃)₂·2H₂O was added into 100 mL DMF, and then, 4 mmol NH₄HF₂ was added followed by 30-min vigorous stirring. The mixture was transferred to a 300 mL Teflon-lined autoclave, and kept under 160 °C for 4 h. After cooling to room temperature, the generated solid nanoparticles were first centrifuged to remove liquid, and sequentially, rinsed with deionized water and ethanol. The cleaned nanoparticles was then dried under vacuum at 60 °C overnight to obtain the desired Cu(OH)F catalyst.

To prepare the electrode for CO₂ reduction to ethylene, 14 mg of the prepared Cu(OH)F catalyst and 20 µL Nafion D520 solution (5 wt%) were added to 1.6 mL isopropanol-tetrahydrofuran solution (1:1 volume ratio). Sonicating the mixture for 30 min to fully disperse Cu(OH)F catalyst particles. The prepared catalyst ink was air-brushed on a gas diffusion electrode (YLS-30T, 3 cm × 3 cm) to prepare the Cu(OH)F-GDE catalyst. In order to further increase the hydrophobicity of the catalyst, 200 µL of 1H,1H,2H,2H-perfluorooctyltrichlorosilane solution (5 wt% in toluene) was painted on the carbon fiber side (i.e., the side without brushed catalyst). Finally, the Cu(OH)F-GDE catalyst was vacuum dried at 30 °C before use.

Procedure for electroreduction of CO₂ to ethylene

For electroreduction of CO₂ to ethylene, Cu(OH)F-GDE catalyst was used as the cathode (5 cm²) and IrO₂-DSA was used as the anode (5 cm²). The catholyte was 150 mL of 2.0 M KOH aqueous solution and anolyte was 150 mL of 1.0 M KOH aqueous solution. Two chamber was separated by an anion exchange membrane (FAB-PK-130), which was activated in 0.5 M K₂CO₃ for 24 h before use. During the electrolysis, 5 sccm of humidified CO₂ controlled by mass flow controllers (CS200-

A, Beijing Sevenstar Flow) continuously flowed into the cathodic gas chamber, and the catholyte and anolyte were both circulated at 5 mL/min flowrate. For the ethylene product analysis, collecting the 0.6 mL gas mixture at the outlet of the cathodic gas chamber using a gas-tight syringe, which was then injected into a gas chromatography system with a thermal conductivity detector (TCD) and flame ionization detector (FID). Each sample was analyzed three times and the averaged result was reported. The FE was calculated as in Eq. (8):

$$FE = \frac{n_a F V_{gas} mol\%_{C2H4}}{Q V_m} \qquad (8)$$

where n_a is the number of electrons transferred for 1 mol C_2H_4 production, V_{gas} is the flow rate of CO_2, $mol\%_{C2H4}$ is the ethylene molar percent in the reactor outlet gas mixture measured via GC, Q is the applied current per unit time, and V_m is the unit molar volume of CO_2.

Cascade electrosynthesis of EC using CO_2 and water

For cascade electrosynthesis of EC using CO_2 and water, the CO_2 electroreduction settings are the same to the aforementioned part. The outlet stream was directly sparged into a batch cell for the subsequent EC electrosynthesis without intermediate purification. 0.2 M Cs_2CO_3, 0.5 M KBr and 3 mM $K_2Cr_2O_7$ dissolved in 3 mL DMF-water blended solution (3:7 volume ratio) was used as the electrolyte in a batch cell and the electrolysis was conducted under 6 mA/cm² using IrO_2-DSA anode materials (size 0.5 cm², 1 mm thick) and nickel foam cathode (0.5 cm², 1 mm thick) for 12 h.

Data availability

The datasets generated and analyzed in this study are included in the main text and supplementary information. Source data are provided with this paper.

References

1. Chen, Y. et al. A review of lithium-ion battery safety concerns: The issues, strategies, and testing standards. *J. Energy Chem.* **59**, 83–99 (2021).
2. Khan, F. M. N. U., Rasul, M. G., Sayem, A. S. M. & Mandal, N. K. Design and optimization of lithium-ion battery as an efficient energy storage device for electric vehicles: A comprehensive review. *J. Energy Storage* **71**, 108033 (2023).
3. Monta, M. & Matsuda, Y. Ethylene carbonate-based organic electrolytes for high performance aluminium electrolytic capacitors. *J. Power Sources* **60**, 179–183 (1996).
4. Bhuyan, Md. S. A. & Shin, H. Green Recovery of Cathode Active Materials from Li-Ion Battery Electrode Scraps Using Propylene Carbonate: A Novel Approach for Direct Recycling. *ACS Sustain. Chem. Eng.* **11**, 10677–10687 (2023).
5. Ethylene Carbonate Market Size. https://www.mordorintelligence.com/industry-reports/ethylene-carbonate-market. (Accessed 2023-12-18).
6. Gu, X., Zhang, X., Zhang, X. & Deng, C. Simulation and assessment of manufacturing ethylene carbonate from ethylene oxide in multiple process routes. *Chin. J. Chem. Eng.* **31**, 135–144 (2021).
7. Pescarmona, P. P. & Taherimehr, M. Challenges in the catalytic synthesis of cyclic and polymeric carbonates from epoxides and CO_2. *Catal. Sci. Technol.* **2**, 2169–2187 (2012).
8. Leow, W. R. et al. Chloride-mediated selective electrosynthesis of ethylene and propylene oxides at high current density. *Science* **368**, 1228–1233 (2020).
9. Service, R. F. Renewable bonds. *Science* **365**, 1236–1239 (2019).
10. De Luna, P. et al. What would it take for renewably powered electrosynthesis to displace petrochemical processes? *Science* **364**, eaav3506 (2019).
11. Zheng, T. et al. Upcycling CO_2 into energy-rich long-chain compounds via electrochemical and metabolic engineering. *Nat. Catal.* **5**, 388–396 (2022).
12. Lee, M. G. Selective synthesis of butane from carbon monoxide using cascade electrolysis and thermocatalysis at ambient conditions. *Nat. Catal.* **6**, 310–318 (2023).
13. Li, K. et al. Enhancement of lithium-mediated ammonia synthesis by addition of oxygen. *Science* **374**, 1593–1597 (2021).
14. Li, Y. et al. Redox-mediated electrosynthesis of ethylene oxide from CO_2 and water. *Nat. Catal.* **5**, 185–192 (2022).
15. Ke, J. et al. Facet-dependent electrooxidation of propylene into propylene oxide over Ag_3PO_4 crystals. *Nat. Commun.* **13**, 932 (2022).
16. Ho, K.-P., Chan, T. H. & Wong, K.-Y. An environmentally benign catalytic system for alkene epoxidation with hydrogen peroxide electrogenerated in situ. *Green Chem.* **8**, 900 (2006).
17. Lee, K. M. et al. Redox-neutral electrochemical conversion of CO_2 to dimethyl carbonate. *Nat. Energy* **6**, 733–741 (2021).
18. Chiarotto, I., Mattiello, L. & Feroci, M. The Electrogenerated Cyanomethyl Anion: An Old Base Still Smart. *Acc. Chem. Res.* **52**, 3297–3308 (2019).
19. Niu, D. et al. Synthesis of cyclic carbonates from epoxides and CO_2 in acetonitrile via the synergistic action of BMIMBr and electrogenerated magnesium. *Chin. J. Catal.* **37**, 1076–1080 (2016).
20. Buckley, B. R., Patel, A. P. & Wijayantha, K. G. U. Electrosynthesis of cyclic carbonates from epoxides and atmospheric pressure carbon dioxide. *Chem. Commun.* **47**, 11888–11890 (2011).
21. Gao, X. et al. Efficient conversion of CO_2 with olefins into cyclic carbonates via a synergistic action of I_2 and base electrochemically generated in situ. *Electrochem. Commun.* **34**, 242–245 (2013).
22. Jang, J. H. et al. Electrochemically initiated synthesis of ethylene carbonate from CO_2. *Nat. Synth.* **3**, 846–857 (2024).
23. Dorchies, F. et al. Controlling the Hydrophilicity of the Electrochemical Interface to Modulate the Oxygen-Atom Transfer in Electrocatalytic Epoxidation Reactions. *Chem. Soc.* **144**, 22734–22746 (2022).
24. Jin, K. et al. Epoxidation of Cyclooctene Using Water as the Oxygen Atom Source at Manganese Oxide Electrocatalysts. *J. Am. Chem. Soc.* **141**, 6413–6418 (2019).
25. Tayebi, M. et al. Photoelectrochemical Epoxidation of Cyclohexene on an α-Fe_2O_3 Photoanode Using Water as the Oxygen Source. *ACS Appl. Mater. Interfaces* **15**, 20053–20063 (2023).
26. Miller, J. H., Joshi, A., Li, X. & Bhan, A. Catalytic degradation of ethylene oxide over Ag/α-Al_2O_3. *J. Catal.* **389**, 714–720 (2020).
27. Chung, M. et al. Direct propylene epoxidation via water activation over Pd-Pt electrocatalysts. *Science* **383**, 49–55 (2024).
28. Reithofer, M. R., Sum, Y. N. & Zhang, Y. Synthesis of cyclic carbonates with carbon dioxide and cesium carbonate. *Green Chem.* **15**, 2086–2090 (2013).
29. Ochoa-Gómez, J. R. et al. Synthesis of glycerol carbonate from 3-chloro-1,2-propanediol and carbon dioxide using triethylamine as both solvent and CO_2 fixation–activation agent. *Chem. Eng. J.* **175**, 505–511 (2011).
30. Huang, L. et al. Ethylene Electrooxidation to 2-Chloroethanol in Acidic Seawater with Natural Chloride Participation. *J. Am. Chem. Soc.* **145**, 15565–15571 (2023).
31. Skaff, O., Pattison, D. I. & Davies, M. J. Kinetics of Hypobromous Acid-Mediated Oxidation of Lipid Components and Antioxidants. *Chem. Res. Toxicol.* **20**, 1980–1988 (2007).
32. Wang, Q. et al. Electrocatalytic CO_2 Upgrading to Triethanolamine by Bromine-assisted C_2H_4 Oxidation. *Angew. Chem. Int. Ed.* **62**, e202212733 (2023).

33. Ayers, P. W., Anderson, J. S. M., Rodriguez, J. I. & Jawed, Z. Indices for predicting the quality of leaving groups. *Phys. Chem. Chem. Phys.* **7**, 1918–1925 (2005).

34. Chi, M. et al. Spatial decoupling of bromide-mediated process boosts propylene oxide electrosynthesis. *Nat. Commun.* **15**, 3646 (2024).

35. Grgur, B. N. Electrochemical Oxidation of Bromides on DSA/RuO₂ Anode in the Semi-Industrial Batch Reactor for On-Site Water Disinfection. *J. Electrochem. Soc.* **166**, E50–E61 (2019).

36. Kozak, J. A. et al. Bromine-Catalyzed Conversion of CO₂ and Epoxides to Cyclic Carbonates under Continuous Flow Conditions. *J. Am. Chem. Soc.* **135**, 18497–18501 (2013).

37. Hirose, T. et al. Economical synthesis of cyclic carbonates from carbon dioxide and halohydrins using K₂CO₃. *RSC Adv.* **6**, 69040–69044 (2016).

38. Xue, W. et al. Bromine-Enhanced Generation and Epoxidation of Ethylene in Tandem CO₂ Electrolysis Towards Ethylene Oxide. *Angew. Chem. Int. Ed.* **62**, e202311570 (2023).

39. Roshan, K. R. et al. A computational study of the mechanistic insights into base catalysed synthesis of cyclic carbonates from CO₂: bicarbonate anion as an active species. *Catal. Sci. Technol.* **6**, 3997–4004 (2016).

40. Bobbink, F. D., Gruszka, W., Hulla, M., Das, S. & Dyson, P. J. Synthesis of cyclic carbonates from diols and CO₂ catalyzed by carbenes. *Chem. Commun.* **52**, 10787–10790 (2016).

41. Fortier, S. M. An on-line experimental/analytical method for measuring the kinetics of oxygen isotope exchange between CO₂ and saline/hypersaline salt solutions at low (25–50 °C) temperatures. *Chem. Geol.* **116**, 155–162 (1994).

42. Hashemi, S. M. H. et al. A versatile and membrane-less electrochemical reactor for the electrolysis of water and brine. *Energy Environ. Sci.* **12**, 1592–1604 (2019).

43. Esposito, D. V. Membraneless Electrolyzers for Low-Cost Hydrogen Production in a Renewable Energy Future. *Joule* **1**, 651–658 (2017).

44. Li, X.-Y. et al. Mechanism of Cations Suppressing Proton Diffusion Kinetics for Electrocatalysis. *Angew. Chem. Int. Ed.* **62**, e202218669 (2023).

45. Zhang, X. et al. Electrochemical oxygen reduction to hydrogen peroxide at practical rates in strong acidic media. *Nat. Commun.* **13**, 2880 (2022).

46. Endrődi, B., Simic, N., Wildlock, M. & Cornell, A. A review of chromium(VI) use in chlorate electrolysis: Functions, challenges and suggested alternatives. *Electrochimica Acta* **234**, 108–122 (2017).

47. Lindbergh, G. & Simonsson, D. Inhibition of cathode reactions in sodium hydroxide solution containing chromate. *Electrochimica Acta* **36**, 1985–1994 (1991).

48. Biesinger, M. C. et al. Resolving surface chemical states in XPS analysis of first row transition metals, oxides and hydroxides: Cr, Mn, Fe, Co and. *Ni. Appl. Surf. Sci.* **257**, 2717–2730 (2011).

49. Wagner, C. The Cathodic Reduction of Anions and the Anodic Oxidation of Cations. *J. Electrochem. Soc.* **101**, 181 (1954).

50. Tilak, B. V., Viswanathan, K. & Rader, C. G. On the Mechanism of Sodium Chlorate Formation. *J. Electrochem. Soc.* **128**, 1228 (1981).

51. Gallardo-Fuentes, S. et al. On the mechanism of CO₂ electrocycloaddition to propylene oxides. *J. CO2 Util.* **16**, 114–120 (2016).

52. Xiao, Y., Chen, B.-L., Yang, H.-P., Wang, H. & Lu, J.-X. Electrosynthesis of enantiomerically pure cyclic carbonates from CO₂ and chiral epoxides. *Electrochem. Commun.* **43**, 71–74 (2014).

53. Iglesias, D. et al. Multi-step oxidative carboxylation of olefins with carbon dioxide by combining electrochemical and 3D-printed flow reactors. *Green Chem.* **25**, 9934–9940 (2023).

54. Wu, L., Yang, H., Wang, H. & Lu, J. Electrosynthesis of cyclic carbonates from CO₂ and epoxides on a reusable copper nanoparticle cathode. *RSC Adv.* **5**, 23189–23192 (2015).

55. Fan, L. et al. Selective production of ethylene glycol at high rate via cascade catalysis. *Nat. Catal.* **6**, 585–595 (2023).

56. Ethylene price trend and forecast. https://www.procurementresource.com/resource-center/ethylene-price-trends. (Accessed 2024-12-28)

57. Ethylene carbonate price trend and forecast. https://www.procurementresource.com/resource-center/ethylene-carbonate-price-trends. (Accessed 2024-12-28)

58. Flores-Granobles, M. & Saeys, M. Minimizing CO₂ emissions with renewable energy: a comparative study of emerging technologies in the steel industry. *Energy Environ. Sci.* **13**, 1923–1932 (2020).

59. Ma, W. et al. Electrocatalytic reduction of CO₂ to ethylene and ethanol through hydrogen-assisted C–C coupling over fluorine-modified copper. *Nat. Catal.* **3**, 478–487 (2020).

60. Cao, J.-W. et al. One-step ethylene production from a four-component gas mixture by a single physisorbent. *Nat. Commun.* **12**, 6507 (2021).

61. Ren, T., Patel, M. & Blok, K. Olefins from conventional and heavy feedstocks: Energy use in steam cracking and alternative processes. *Energy* **31**, 425–451 (2006).

62. Kim, D. et al. Single-step ethylene purification from ternary C₂ hydrocarbon mixtures in a scalable metal–organic framework. *Chem. Eng. J.* **470**, 143858 (2023).

63. Jiang, Y. et al. Benchmark single-step ethylene purification from ternary mixtures by a customized fluorinated anion-embedded MOF. *Nat. Commun.* **14**, 401 (2023).

64. Chuah, C. Y. Membranes for Gas Separation and Purification Processes. *Membranes* **12**, 622 (2022).

65. Ma, S. One-step electrosynthesis of ethylene and ethanol from CO₂ in an alkaline electrolyzer. *J. Power Sources.* **301**, 219 (2016).

Acknowledgements

Author contributions

Y.M. supervised the project. Y.M. and M.C. conceived the project and designed the experiments. M.C. conducted the experiments as well as performed the technoeconomic analysis. M.C. and Y.M. analyzed the data and prepared the manuscript. Y.M., S.D. and J.X. contributed to the manuscript editing. All the authors discussed the results and assisted during the manuscript preparation.

Competing interests

The authors declare no competing interests.

Additional information

Supplementary information The online version contains supplementary material available at https://doi.org/10.1038/s41467-025-58558-z.

Correspondence and requests for materials should be addressed to Yiming Mo.

Peer review information *Nature Communications* thanks Hussain Almajed, Omar Guerra Fernández, and the other, anonymous, reviewers for their contribution to the peer review of this work. A peer review file is available.

Reprints and permissions information is available at http://www.nature.com/reprints

Publisher's note Springer Nature remains neutral with regard to jurisdictional claims in published maps and institutional affiliations.